Supplementary Figure 1

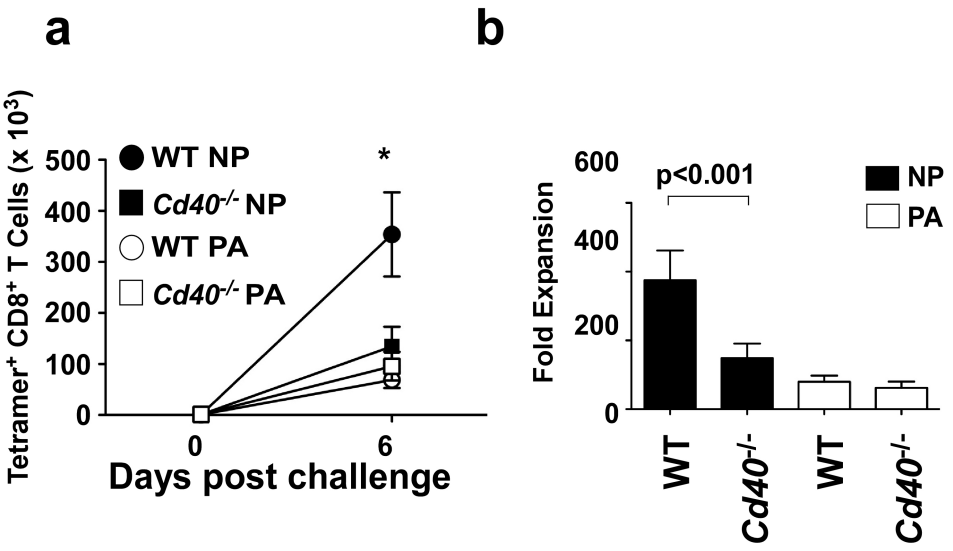

Figure S1, related to Figure 2. Defective NP-specific memory CD8$^+$ T cell responses in the CD40 deficient mice. WT and *Cd40*$^{-/-}$ mice were infected with PR8 and challenged with X31 100 days later. **(a)** Total numbers of NP-specific and PA-specific CD8$^+$ T cells in the mLN. **(b)** Relative expansion of NP- and PA-specific CD8$^+$ T cells in the mLN of C57BL/6 and *Cd40*$^{-/-}$ mice was calculated on day 7 after challenge Data are representative of three independent experiments (mean ± s.d of 5 mice per group). Asterisks indicate statistically significant differences ($p<0.005$).

Supplementary Figure 2

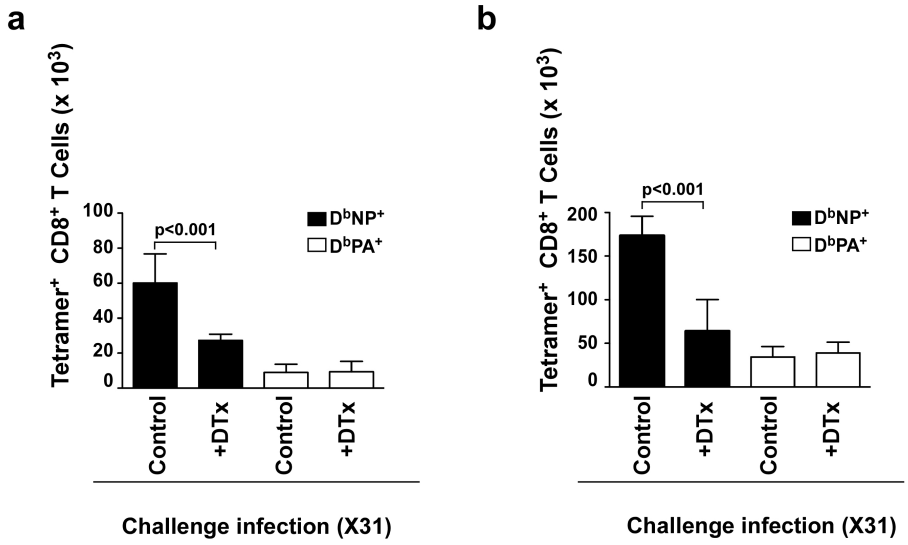

Figure S2, related to Figure 4. NP and PA-specific memory CD8$^+$ T cells in the mLN and spleen of CD11c-DTR-EGFP bone-marrow chimaeras. CD11c-DTR-EGFP bone marrow chimeras were infected with PR8, injected i.p. with PBS or 60 ng DTX every three days between day 6 and 40. Two weeks later, mice were challenged with X31 and the numbers of NP-specific and PA-specific CD8$^+$ T cells were enumerated by flow cytometry in mLN **(a)** and spleen **(b)** 6 days later. Data are representative of two independent experiments (mean ± s.d of 4-5 mice per group). All P values were calculated using a two-tailed Student's t-test.

Supplementary Figure 3

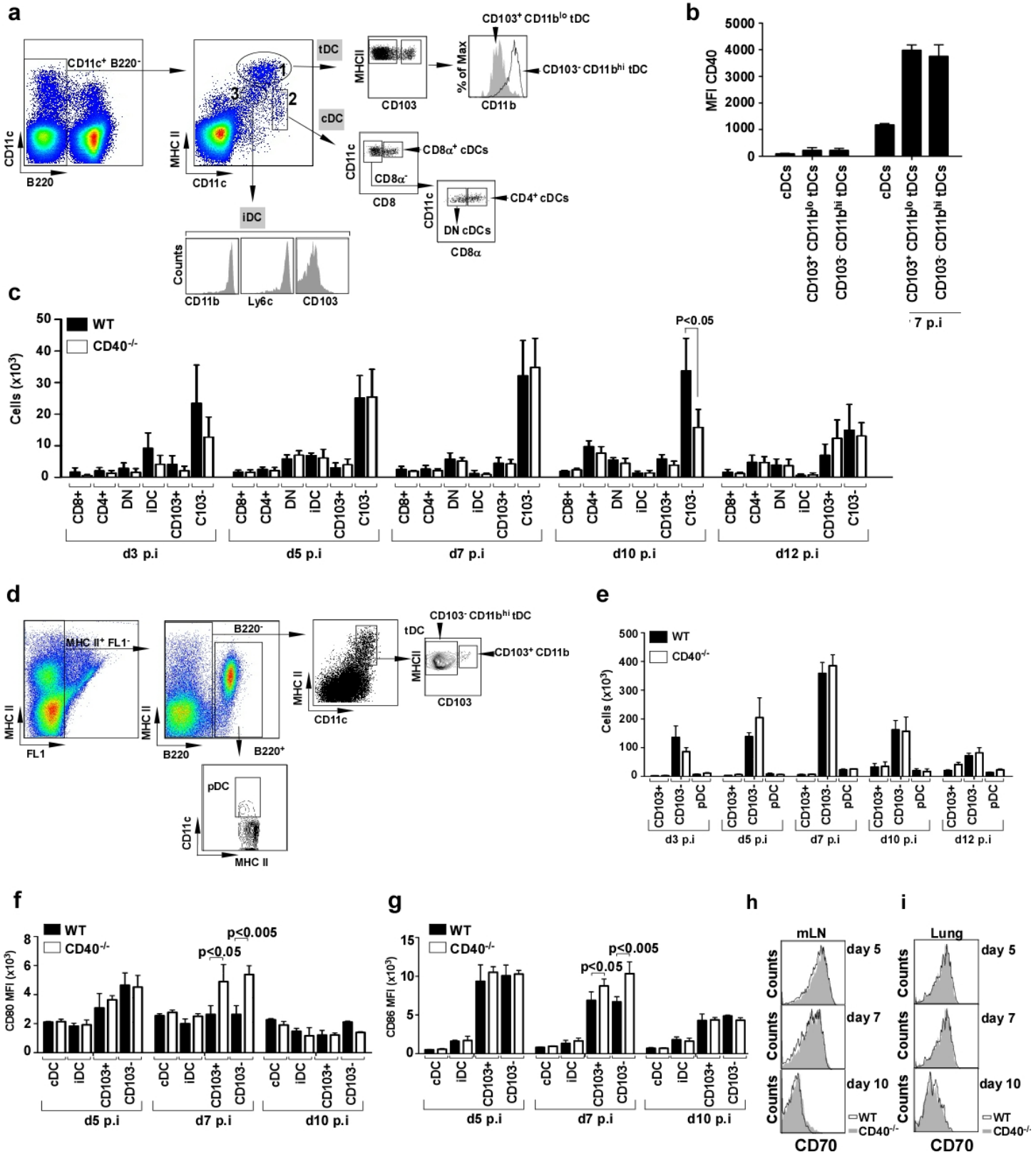

Figure S3, related to Figure 5. Dendritic cell subsets in the mLN. (a) Mice were infected intranasally with PR8 and DC subsets were analyzed by flow cytometry on day 5 after infection. Plasmacytoid DCs were excluded based on B220 expression and the three major subsets that remained were defined as conventional

DCs (cDCs: MHCII^{med}CD11c^{high}), tissue DCs (tDCs: MHCII^{high}CD11c^{med}) and inflammatory DCs (iDCs: MHCII^{med}CD11c^{med}Ly6c^{high}). Each of these populations was further characterized based on the expression of CD8α, CD4, CD103, CD11b and Ly6C. **(b)** Expression of CD40 on cDCs, and CD103^{-}CD11b^{+} and CD103^{+}CD11b^{-} tDC in the mLN of C57BL/6 mice uninfected and infected with PR8. MFI, mean fluorescence intensity Data are representative of two independent experiments (mean ± s.d of 4-5 mice per group). **(c)** Total number of CD8α^{+} cDCs, CD4^{+}CD8α^{-} cDC, CD4^{-}CD8α^{-} cDC, iDCs, CD103^{+}CD11b^{-} tDC and CD103^{-}CD11b^{+} tDC in the mLN of C57BL/6 and *Cd40*$^{-/-}$ mice infected with PR8. DCs were characterized as in a. Data are representative of three independent experiments (mean ± s.d of 4-5 mice per group). **(d)** C57BL/6 mice were infected with PR8 and DC subsets in the lung were analyzed by flow cytometry on day 12 after infection. Autofluorescent cells were excluded from the analysis. Plasmacytoid DCs were subsequently defined as auto^{low}B220^{+}MCHII^{+}CD11c^{+}. The remaining DCs were divided based on the expression of CD103 and CD11b. **(e)** Total number of CD103^{+}CD11b^{-} tDC, CD103^{-}CD11b^{+} tDC and plasmacitoyd DCs in the lungs of C57BL/6 and *Cd40*$^{-/-}$ mice infected with PR8. DCs were characterized as in a. Data are representative of two independent experiments (mean ± s.d of 4-5 per group). Expression of CD80 (**f**) and CD86 (**g**) on DCs subsets in the mLN of C57BL/6 and *Cd40*$^{-/-}$ mice infected with PR8. MFI, mean fluorescence intensity. Data are representative of two independent experiments (mean ± s.d of 4-5 mice per group). **(h and i)** Expression of CD70 on CD103^{-} CD11b^{+} tDC in the mLN (**h**) or lung (**i**) of C57BL/6 and *Cd40*$^{-/-}$ mice infected intranasally with PR8. Data are representative of three independent experiments (4-5 mice per group). All P values were calculated using a two tailed Student's t-test